Published in final edited form as:
J Bone Miner Res. 2012 November ; 27(11): 2314–2324. doi:10.1002/jbmr.1693.

Distribution of bone density in the proximal femur and its association with hip fracture risk in older men: the MrOS Study

Lang Yang[1,2], **Annabel C Burton**[2], **Mike Bradburn**[3], **Carrie M Nielson**[4], **Eric S Orwoll**[4], and **Richard Eastell**[1,2] **for the Osteoporotic Fractures in Men (MrOS) Study Group**

Lang Yang: l.yang@sheffield.ac.uk; Annabel C Burton: annabelb85@googlemail.com; Mike Bradburn: m.bradburn@sheffield.ac.uk; Carrie M Nielson: nielsoca@ohsu.edu; Eric S Orwoll: orwoll@ohsu.edu; Richard Eastell: r.eastell@sheffield.ac.uk

[1]NIHR Biomedical Research Unit for Musculoskeletal Disease, Sheffield Teaching Hospitals NHS Foundation Trust, Sheffield, UK

[2]Academic Unit of Bone Metabolism, University of Sheffield, Sheffield, UK

[3]Clinical Trials Research Unit, School of Health and Related Research, University of Sheffield, Sheffield, UK

[4]Bone and Mineral Unit, Oregon Health & Science University, Portland Oregon, USA

Abstract

This prospective case-cohort study aimed to map the distribution of bone density in the proximal femur and examine its association with hip fracture. We analyzed baseline quantitative computed tomography (QCT) scans in 250 men aged 65 yrs or older, which comprised a randomly-selected subcohort of 210 men and 40 cases of first hip fracture during a mean follow-up period of 5.5 yr. We quantified cortical, trabecular and integral vBMD and cortical thickness (CtTh) in four quadrants of cross sections along the length of the femoral neck (FN), intertrochanter (IT) and trochanter (TR). In most quadrants, vBMDs and CtTh were significantly ($P<0.05$) lower in cases compared to the subcohort and these deficits were present across the entire proximal femur. To examine the association of QCT measurements with hip fracture, we merged the two quadrants in the medial and lateral aspects of the FN, IT and TR. At most sites, QCT measurements were associated significantly ($p<0.001$) with hip fracture, the hazard ratio (HR) adjusted for age, BMI and clinical site for one standard deviation decrease ranged between 2.28 (95% CI 1.44–3.63) to 6.91 (95% CI 3.11–15.53). After additional adjustment for TH aBMD, trabecular vBMDs at the FN, TR and TH were still associated with hip fracture significantly ($p<0.001$), the HRs ranged from 3.21 (95% CI 1.65–6.24) for the supero-lateral FN to 6.20 (95% CI 2.71–14.18) for medial TR. QCT measurements alone or in combination did not predict fracture significantly ($p>0.05$) better than TH aBMD. With an AUC of 0.901 (95% CI 0.852–0.950), the regression model combining TH aBMD, age and trabecular vBMD predicted hip fracture significantly ($p<0.05$) better than TH aBMD alone or TH aBMD plus age. These findings confirm that both cortical and trabecular bone contribute to hip fracture risk and highlight trabecular vBMD at the FN and TR as an independent risk factor.

Corresponding author: Dr. Lang Yang, School of Medicine and Biomedical Sciences, Beech Hill Road, Sheffield S10 2RX, UK, Tel: +44 114 2714705; Fax: +44 114 2618775; L.Yang@sheffield.ac.uk.

CONFLICT OF INTEREST

All authors stated that they have no conflict of interest.

Introduction

The mechanical competence of bone is determined by its size and shape, and by the spatial distribution, organization and intrinsic properties of the bone tissue [1–3]. Areal bone mineral density (aBMD) measured by dual-energy x-ray absorptiometry (DXA) explains 50% to 80% of the mechanical strength of bone *in vitro* [4–6] and is strongly associated with clinical fractures [7,8], but it does not reflect the three-dimensional distribution of bone mass, cortical and trabecular microarchitecture and intrinsic properties of the bone matrix. Quantitative computed tomography (QCT), on the other hand, measures cortical volumetric BMD (vBMD), trabecular vBMD, bone volume, cross-sectional area and cortical thickness [5,9–13]. For these reasons, QCT has become an important clinical research tool that has been used to examine age-related changes [10,11,14–16], effects of drug therapy[17–19], mechanical unloading in the proximal femur[20] and association of femoral bone structure and strength with hip fracture [4,21–27]. In most such QCT studies, cortical, trabecular and integral vBMD was measured in the whole femoral neck (FN), intertrochanter (IT), trochanter (TR) and total hip (TH). Other structural measures, such as moment of inertia, cortical thickness and buckling ratio have also been estimated in certain but not all cross-sections of the FN, trochanter and femoral shaft. Age-related bone loss has been found to be predominately on the superior aspect of the FN [10,11,28] and patients with fractured neck of femur have thinner cortex than those without fracture, particularly on the inferior aspect of the FN [29,30]. It is unclear whether there are such differences in other regions of the proximal femur.

The purpose of this study was to map the distribution of bone density in the proximal femur of older men and examine its association with hip fracture.

Materials and Methods

Study population and cohort selection

The MrOS study enrolled 5995 men from six US cities, from March 2000 through April 2002 as previously described [31]. Eligible participants were ≥65 yr of age, able to walk without assistance, and had not had bilateral hip replacement surgery. At baseline, participants had aBMD measured at the hip by DXA (QDR 4500W, Hologic Inc., Bedford, USA) and measurements of weight and height. A subset of 3633 participants (61% of the MrOS cohort) also had QCT of the hip at baseline. Questionnaires were mailed to participants every 4 months to obtain information about recent fractures. Reported hip fractures were validated by physician review of the radiology report or radiographs.

For this analysis we adopted a case-cohort design [32]. Using a random selection procedure we selected 225 men from the 3663 participants with QCT to form the subcohort of the case-cohort. Forty-one incident hip fractures occurred as of February 2007 (average follow-up of 5.5 yr) in men with available baseline QCT and 4 were in the subcohort. Sixteen participants were excluded from the analysis due to poor image quality, leaving 250 in the final analysis (210 no fracture, 40 cases).

Quantitative computed tomography

The acquisition of QCT scans has been described previously [14]. Briefly, participants were positioned supine and the pelvic region was scanned from just above the femoral head to 3.5 cm below the lesser trochanter. During scanning, a density calibration phantom (Image Analysis, Columbia KY, USA) was placed beneath the patient between the hips. Scan parameters were 3-mm section thickness, 80 kVp, 280 mA, and 512×512 matrix in spiral reconstruction, with an in-plane pixel size of 0.94 mm. The CT images were archived to DICOM CD-ROM for further analysis.

Three-dimensional structural analysis of the hip

We analysed the left hip scans, and researchers (AB & LY) who performed the analysis were blinded to who had incident hip fracture. As an post-hoc analysis we also analyzed 37 out of 40 right hips of men with incident hip fracture (3 right hips, all non-fractured side, were partly out of the QCT field of view) and compared the fractured side (n=40) with the un-fractured side (n=37) for men with incident hip fracture.

We developed a suite of Matlab programs (The Mathworks Inc., Natick, MA, USA) to analyse the QCT scans; this has been described previously [13,33]. The Hounsfield Unit of each voxel was converted to mineral density using the density calibration phantom. The outer contours of the proximal femur were determined slice-by-slice using an interactive program that combines density-thresholding at 100 mg/cm^3, morphological operation and manual tracing. From this point onwards, all image processing and calculations were performed automatically. The femoral neck and shaft axes were identified and the femora were digitally rotated to a standard orientation using nearest interpolation so that the FN and shaft axes were in the frontal plane. A series of cross-sections were defined from proximal to distal and perpendicular to the FN axis in the FN and perpendicular to the femoral shaft axis in the IT and TR. The cross sectional images were enlarged by 4 times using bilinear interpolation. The cross sections were further divided into 4 quadrants, namely the infero-anterior (IA), supero-anterior (SA), supero-posterior (SP) and infero-posterior (IP) quadrants for the FN and medio-anterior (MA), latero-anterior (LA), latero-posteiror (LP) and medio-posterior (MP) quadrants for the IT and TR (Figure 1). The quadrant origin was at the geometrical centre of the cross section except for the cross sections in the IT where the origin was defined by the femoral shaft axis. The IT cross-sections were not complete medially since they were bounded by the femoral neck. A 22° rotation of the axes of the FN cross-sections was introduced to account for the incident angle of the femoral anterior surface at stance phase [34]. A 15° external rotation of the axes of the trochanter cross-sections was introduced to account for the femoral neck anteversion (clockwise rotation in Figure 1C and 1D). To define cortical bone in each cross section, we developed and validated a method specifically for clinical hip QCT scans with an in-plane pixel resolution of about 1 mm [33] (see Appendix for details). A threshold of 100 mg/cm^3 was used to identify trabecular bone and exclude marrow. For each quadrant of each cross section we calculated cortical, trabecular and integral bone mineral content, bone volume, vBMD and cortical thickness as described previously [13,33]. We used these cross sectional data by quadrants to investigate density distribution. To account for differences in the number of cross sections for different men, we normalised the measurements by interpolating each measurement linearly along the FN, IT and TR and obtained values at 2% length intervals from the proximal to distal.

To determine the association between QCT measurements and hip fracture, we calculated cortical, trabecular and integral vBMDs and averaged cortical thickness for the infero-medial (infero-anterior plus infero-posterior) and supero-lateral (supero-anterior plus supero-posterior) halves of the FN and medial (medio-anterior plus medio-posterior) and lateral (latero-anterior plus latero-posterior) halves of the IT and TR. The justification for this was the apparent differences in loading conditions and cortical bone distribution: the medial side of the femur is mainly in tension in a sideways fall and has a thicker cortex, whereas the lateral side is in compression and the cortex is thinner[10,11,28,35–38]. We also calculated vBMDs, cortical thickness (CtTh), cross sectional area (CSA) and polar moment of inertia (PMI) at the whole FN, whole IT and whole TR and vBMDs only at the whole proximal femur. A total of 46 QCT measurements were examined for their association with hip fracture.

We assessed the intra-observer reproducibility of the analysis by analysing 16 randomly selected scans three times. The coefficients of variation were 0.6–2.5% for vBMD, 1.1–4.9% for cortical thickness, 0.6–1.0% for CSA and 3.3–6.5% for PMI (Table 1).

Statistical analysis

We used the two sample t-test to compare the means for each measurement at each 2% length interval of the interpolated data between the fracture cases and subcohort. We tested the association between hip fracture and QCT measurements by performing Cox proportional hazard regression; the time to incident hip fracture was modelled with Prentice weighting and robust variance estimation (as recommended for case-cohort analysis) [(32)]. Each QCT measurement was included in a separate model of time to first hip fracture to estimate the relative increase in hazard of hip fracture for 1 standard deviation change in its value. Age, BMI, clinical site and TH aBMD were sequentially added to the regression model to assess their effects on the hazard ratio (HR). To account for multiple comparisons of 46 variables, we set statistical significance level for HR at 0.001 based on Bonferroni correction. To examine the ability of QCT measurements to predicting incident hip fracture, we performed stepwise logistic regression that included the QCT measurements only, the QCT measurements plus age and the QCT measurements plus age and TH aBMD. The ability of the resulting multi-covariate regression models to predict incident fracture were compared in terms of the area under the ROC curve (AUC) against the models that included TH aBMD alone and TH aBMD plus age.

Results

Baseline characteristics

The baseline characteristics of the subcohort were very similar to the whole MrOS cohort (Table 2), confirming the validity of the random selection. Participants in the case group were significantly older and lighter and with significantly lower TH aBMD (Table 2).

Volumetric BMD

The patterns of variation in vBMD along the FN were similar for both the case and subcohort (Figure 2). Volumetric BMDs in quadrants were more or less constant from proximal to distal (variation in mean vBMD less than 0.10 g/cm^3 and 40%) except for cortical and integral vBMDs in the infero-medial (IA and IP) quadrants of the FN that increased markedly from the proximal to the distal (average increases of 0.46 g/cm^3 or 154% and 0.24 g/cm^3 or 78% in cortical and integral vBMD, respectively). On average, cortical and trabecular vBMDs in the infero-medial (IA and IP) quadrants were 95% and 54% higher than those in the supero-lateral (SA and SP) quadrants ($p<0.001$), respectively. In comparison to men in the subcohort, case group had significantly ($p<0.05$) lower cortical, trabecular and integral vBMD in all quadrants and along the most of the FN length. Averaged vBMD over quadrant was 10% to 20% lower in case group compared to subcohort ($P<0.001$).

Figure 3 shows bone density distribution in the intertrochanter for both cases and subcohort. Intertrochanteric vBMD was not measured in the proximal 10% of the medial (MA and MP) quadrants because these regions did not contain any bone. Cortical vBMD in all quadrants increased from proximal to distal, 0.55 g/cm^3 or 260% on average in the anterior (MA and LA) quadrants and 0.21 g/cm^3 or 76% on average in the posterior (MP and LP) quadrants. Trabecular and integral vBMD were lowest in the central third of the intertrochanter. Cortical and integral vBMD was 7% to 19% lower in case group compared to sub cohort ($P<0.001$) except for integral vBMD in MA quadrant.

At the trochanter, cortical vBMD changed little from proximal to distal in the MA and MP quadrants, whereas it increased in the LA and LP quadrants by 0.29 g/cm^3 or 55% on average for both cases and subcohort (Figure 4). The highest cortical vBMD was in the MA, and the lowest vBMD was in the MP quadrant (which includes the lesser trochanter). Unlike the cortical and integral measurements, trabecular vBMD did not differ significantly between groups except in the MP quadrant, where it was 18% lower in men with fracture (P<0.000).

Cortical thickness

For both cases and subcohort, cortical thickness increased from <1 mm proximally to over 3 mm distally in the infero-medial (IA and IP) quadrants of the FN and the anterior (MA and LA) qradrants of the intertrochanter, whereas it remained <1.0 mm in the superior (SA and SP) quadrants of the FN and the MP quadrant of the intertrochanter (Figure 5). In the trochanter, cortical thickness was always greater than 2 mm in the anterior (MA and LA) quadrants with changes around 1 mm along the length: decreases in MA and increased in LA quadrants. It increased in LP from 1.5 mm to 3–5 mm, whereas it remained at 1 to 1.5 mm in the MP quadrant.

Men in the case group had significantly thinner cortex than the subcohort throughout the proximal femur and the percentage differences in mean thickness ranged from 14% to 30%.

Cross sectional area and polar moment of inertia

Mean cross sectional area of the fracture cases was 12.9 (95% CI 12.3, 13.5) cm^2 at the FN, 18,2 (17.2, 19.3) cm^2 at the IT and 20.7 (19.7, 21.8) cm^2 at the TR, which were not significantly greater than the subcohort's values of 12.4 (95% CI 12.1, 12,6) cm^2 at the FN (p=0.09), 17.2 (16.8, 17.6) cm^2 at the IT (p=0.06) but significantly larger than 19.5 (19.1, 20.0) cm^2 at the TR (p=0.04), respectively. Polar moment of inertia at the FN was significantly (p=0.001) lower in cases (mean 47.4, 95% CI 41.2–53.6 cm^4) than in the subcohort (mean 60.2, 95% CI 55.9–64.6 cm^4), whereas they were similar at the IT (mean=492, 95% CI 419–567 v. mean 569, 95% CI 529–610 cm^4, p=0.07) and TR (mean 375, 95% CI 337–413 v. mean 384, 95% CI 365–404, p=0.66).

Associations with hip fracture

Hazard ratios for one standard deviation increase in age and decreases in BMI and TH aBMD were 2.69 (95% CI 1.79–4.04), 1.46 (95% CI 1.00–2.14) and 5.18 (95% CI 2.76–9.72), respectively.

Table 3 shows the hazard ratio (HR) of incident hip fracture, adjusted for age, BMI and clinical site, for one standard deviation decrease in vBMD, cortical thickness and PMI and one standard deviation increase in PMI. Significance level for HR was set at 0.001, the Bonferroni-corrected alpha for multiple comparison. Except cortical vBMD at the infero-medial FN and trabecular and integral vBMDs at the medial IT, all vBMDs at the FN and IT were significantly associated with hip fracture, the HR adjusted for age, BMI and clinical site for one standard deviation decrease ranged between 2.28 (95% CI 1.44–3.63) for cortical vBMD at the medial IT to 6.54 (95% CI 3.35–12.77) for trabecular vBMD at the whole FN (Table 3). At the TR, trabecular and integral vBMDs at the medial side and cortical and integral vBMDs at the whole TR were significantly associated with hip fracture whereas all vBMDs at the lateral side were not. Cortical thickness in all regions but the supero-lateral FN was significantly associated with hip fracture. The vBMD and cortical thickness at the lateral sides of the FN and IT had higher HRs than the medial side, whereas trabecular vBMD at the whole FN and IT had the highest HRs. However, these differences

were not statistically significant ($p>0.05$). Cross sectional area and polar moment of inertia were not significantly associated with hip fracture.

After adjustment for age, BMI, clinical site and total hip aBMD, trabecular vBMDs at the medial, lateral and whole FN, medial TR, whole TR and total hip were still associated with hip fracture significantly, the HRs ranged from 3.21 (95% CI 1.65–6.24) for the supero-lateral FN to 6.20 (95% CI 2.71–14.18) for medial TR (Table 4).

TH aBMD alone predicted hip fracture with a AUC of 0.829 (95% CI 0.756–0.902) and adding age improved the prediction slightly (AUC 0.863, 95% CI 0.797–0.929). QCT parameters alone or in combination did not predict fracture significantly better than TH aBMD alone, the AUC ranged from 0.675 (95 CI 0.577–0.773) for cortical vBMD at the infero-medial FN to 0.880 (95% CI 0.832–0.929) for a regression model that included trabecular vBMDs at the superolateral FN, medial IT and medial TR. A regression model combining age and trabecular vBMD at the superolateral FN and medial TR had a AUC of 0.896 (95% CI 0.849–0.944), which was significantly larger than that of TH aBMD alone but not significantly greater than TH aBMD plus age. Adding TH aBMD to the model produced a AUC of 0.901 (95% CI 0.852–0.950), which was significantly ($p<0.005$) larger than TH aBMD alone and TH aBMD plus age.

Comparion between fractured and contra-lateral sides

All QCT measures were not significantly ($p>0.12$) different between the fractured and contra-lateral side for men who sustained an incident hip fracture (Table 5).

Discussion

In this prospective case-cohort study we used QCT to quantify the distribution of bone density in the proximal femur of older men with and without incident hip fracture. We measured cortical, trabecular and integral vBMD and cortical thickness in four quadrants of all cross sections and examined the pattern of their variations along the femoral neck, intertrochanter and trochanter. No other studies have described these so comprehensively. We found that although the pattern of bone density distribution was similar in men with and without hip fracture, there were significant deficits in vBMD and cortical thickness in men with hip fracture which existed not only in the FN but also other regions of the proximal femur. Lower vBMD and cortical thickness in the FN, intertrochanter and trochanter were all significantly associated with hip fracture, but only trabecular vBMD at the FN and medial aspect of the trochanter predicted hip fracture independently of areal BMD, age and BMI.

The relative contribution of cortical and trabecular bone to the femoral strength and hip fracture risk is important for understanding bone fragility and effects of therapeutic treatment of osteoporosis. Mechanical testing of *ex vivo* specimens and finite element analysis demonstrate that both cortical and trabecular bone contribute to femoral strength proportionate to their mass [4,36,38,39]. Cortical and trabecular vBMD at the femoral neck decline with age [11,15,40] and are associated with hip fracture [4,23–27]. We confirmed in this study that there are significant deficits in both cortical and trabecular vBMD in men with hip fracture across the whole of the proximal femur. We demonstrated that while the vBMD deficit was more widely present in the cortical than the trabecular compartments (particularly in the intertrochanter and trochanter), the percentage differences in mean vBMD between those with and without hip fracture over the whole quadrant were similar in both compartments. Furthermore, the hazard ratios for cortical and trabecular vBMD were statistically similar after adjusting for age, BMI and study site. These results suggest that

both cortical and trabecular bone deficits across the whole proximal femur contribute to the bone fragility and hip fracture risk.

In vivo and *in vitro* analyses of a standard region of the femoral neck show that age-related cortical thinning is concentrated in the supero-lateral aspect [10,11], whereas in patients with fracture, the cortex is mainly thinner in the infero-medial aspect [29,30,41]; the thinner cortex is probably due to increased cortical remodelling and trabecularization [42,43] in that region. Our femoral neck data corroborate the evidence from these studies. Furthermore, we also observed significantly thinner cortex at the intertrochanter and trochanter in men with than men without incident hip fracture, which suggests that cortical remodelling and trabecularization is not limited to the femoral neck and occurs throughout the proximal femur.

Some QCT studies report better prediction of hip fracture risk using QCT measures in combination with aBMD [4,26] compared to aBMD alone, but this was not replicated in all studies [25,44]. Our results support the rationale for using vBMD measured by QCT, as the latter includes separate measurements of the cortical and trabecular compartments and thus captures information that is more relevant to bone strength. However, the improvement over aBMD was not large enough to justify substituting QCT for DXA in wider clinical use due to very small improvement in prediction with the combination of DXA and QCT measures versus DXA alone, the limited availability of QCT, the higher radiation dose and the higher financial cost compared to DXA. On the other hand, QCT is valuable as a research tool to promote better understanding of the pathophysiology of hip fracture and to monitor the treatment effects of osteoporosis drugs. In addition to bone measurements, QCT can also be used to assess other factors that may influence the risk of hip fracture. These include factors related to physical function (such as muscle cross-sectional area and adiposity) or to impact force attenuation (such as trochanteric soft tissue thickness for example) [45,46],[47].

Our study had some limitations. The study population was small in relation to the number of variables studied that precludes analysis of femoral neck and extracapsular fractures separately. Secondly, there is an inherent limitation to the accuracy of cortical vBMD and thickness measurement using QCT, particularly at the superolateral aspect of the FN where cortex is thin. Hangartner and Gilsanz [48] demonstrated that, with a pixel size of 0.6×0.6 mm and true cortical thickness of 1 mm, cortical vBMD could be under-estimated by 30% and cortical thickness overestimated by 70% using the full width half maximum method. Prevrhal et al [49] pointed out that oblique orientation of bone surface relative to the CT acquisition plane causes further overestimation of cortical thickness. We estimated cortical thickness using a density-weighted method that took into account the influence of partial volume effects to some extent and our results are comparable with others obtained using higher resolution QCT [11,26]. However, the effect of bone surface orientation was not accounted for. Futhermore, we digitally rotate the femur in a standard orientation by interpolation, which may affect the QCT measurements. However, limitations in accuracy should have little effect on the significant differences between hip fracture cases and non-cases. Recently Treece et al [12] developed a method to accurately measure the femoral cortical thickness with QCT and map the thickness to cortical surface, and Poole et al [50] demonstrated its value in examine the effect of PTH treatment for several osteoporosis. Finally, this study was performed in a largely white, male population, so the results may not be fully generalizable to other populations.

In conclusion, we examined the patterns of variation in cortical and trabecular bone density and cortical thickness in the proximal femur comprehensively and found they were similar between hip fracture cases and cohorts. However, throughout the proximal femur, bone density and cortical thickness were lower in men who experienced incident fracture

compared with unfractured men. The differences between groups were more frequent in cortical regions, but the percentage differences were similar in both cortical and trabecular compartments. All cortical and trabecular measures at the FN, intertrochanter and trochanter were highly associated with hip fracture after adjustment for clinical site, age and body mass index, and trabecular vBMD in the FN and trochanter were still associated with fracture after further adjustment for total hip aBMD.

Acknowledgments

Funding source

We would like to thank our sponsors, the Medical Research Council and the National Institute for Health Research (NIHR). The views expressed in this publication are those of the author(s) and not necessarily those of the NHS, the NIHR or the Department of Health. Acknowledgements go to the editorial board of the Sheffield NIHR Biomedical Research Unit for Musculoskeletal Deceases for their help in preparing this manuscript.

The MrOS Study is supported by National Institutes of Health funding. The following institutes provide support: the National Institute of Arthritis and Musculoskeletal and Skin Diseases (NIAMS), the National Institute on Aging (NIA), the National Center for Research Resources (NCRR), and NIH Roadmap for Medical Research under the following grant numbers: U01 AR45580, U01 AR45614, U01 AR45632, U01 AR45647, U01 AR45654, U01 AR45583, U01 AR052234, U01 AG18197, U01-AG027810, and UL1 RR024140. Additional support for these analyses was provided by Merck& Co., Eli Lilly, and Amgen and by NIH Grant AR049828.

Reference List

1. Bouxsein ML, Karasik D. Bone geometry and skeletal fragility. Curr Osteoporos Rep. 2006; 4:49–56. [PubMed: 16822403]
2. Burr DB. Bone quality: understanding what matters. J Musculoskelet Neuronal Interact. 2004; 4:184–186. [PubMed: 15615122]
3. Seeman E, Delmas PD. Bone quality--the material and structural basis of bone strength and fragility. N Engl J Med. 2006; 354:2250–2261. [PubMed: 16723616]
4. Bousson V, Le BA, Roqueplan F, Kang Y, Mitton D, Kolta S, Bergot C, Skalli W, Vicaut E, Kalender W, Engelke K, Laredo JD. Volumetric quantitative computed tomography of the proximal femur: relationships linking geometric and densitometric variables to bone strength. Role for compact bone. Osteoporos Int. 2006; 17:855–864. [PubMed: 16547689]
5. Lang TF, Keyak JH, Heitz MW, Augat P, Lu Y, Mathur A, Genant HK. Volumetric quantitative computed tomography of the proximal femur: precision and relation to bone strength. Bone. 1997; 21:101–108. [PubMed: 9213015]
6. Lochmuller EM, Muller R, Kuhn V, Lill CA, Eckstein F. Can novel clinical densitometric techniques replace or improve DXA in predicting bone strength in osteoporosis at the hip and other skeletal sites? J Bone Miner Res. 2003; 18:906–912. [PubMed: 12733731]
7. Cummings SR, Black DM, Nevitt MC, Browner W, Cauley J, Ensrud K, Genant HK, Palermo L, Scott J, Vogt TM. Bone density at various sites for prediction of hip fractures. The Study of Osteoporotic Fractures Research Group. Lancet. 1993; 341:72–75. [PubMed: 8093403]
8. Marshall D, Johnell O, Wedel H. Meta-analysis of how well measures of bone mineral density predict occurrence of osteoporotic fractures. BMJ. 1996; 312:1254–1259. [PubMed: 8634613]
9. Genant HK, Engelke K, Prevrhal S. Advanced CT bone imaging in osteoporosis. Rheumatology (Oxford). 2008; 47(Suppl 4):iv9–16. [PubMed: 18556648]
10. Mayhew PM, Thomas CD, Clement JG, Loveridge N, Beck TJ, Bonfield W, Burgoyne CJ, Reeve J. Relation between age, femoral neck cortical stability, and hip fracture risk. Lancet. 2005; 366:129–135. [PubMed: 16005335]
11. Poole KE, Mayhew PM, Rose CM, Brown JK, Bearcroft PJ, Loveridge N, Reeve J. Changing Structure of the Femoral Neck Across the Adult Female Lifespan. J Bone Miner Res. 2009; 25:482–491. [PubMed: 19594320]
12. Treece GM, Gee AH, Mayhew PM, Poole KE. High resolution cortical bone thickness measurement from clinical CT data. Med Image Anal. 2010; 14:276–290. [PubMed: 20163980]

13. Yang L, Maric I, McCloskey EV, Eastell R. Shape, structural properties and cortical stability along the femoral neck: a study using clinical QCT. J Clin Densitom. 2008; 11:373–382. [PubMed: 18550404]

14. Marshall LM, Lang TF, Lambert LC, Zmuda JM, Ensrud KE, Orwoll ES. Dimensions and Volumetric BMD of the Proximal Femur and Their Relation to Age Among Older U.S. Men. J Bone Miner Res. 2006; 21:1197–1206. [PubMed: 16869717]

15. Riggs BL, Melton IL III, Robb RA, Camp JJ, Atkinson EJ, Peterson JM, Rouleau PA, McCollough CH, Bouxsein ML, Khosla S. Population-based study of age and sex differences in bone volumetric density, size, geometry, and structure at different skeletal sites. J Bone Miner Res. 2004; 19:1945–1954. [PubMed: 15537436]

16. Keaveny TM, Kopperdahl DL, Melton LJ III, Hoffmann PF, Amin S, Riggs BL, Khosla S. Age-dependence of femoral strength in white women and men. J Bone Miner Res. 2010; 25:994–1001. [PubMed: 19874201]

17. Black DM, Greenspan SL, Ensrud KE, Palermo L, McGowan JA, Lang TF, Garnero P, Bouxsein ML, Bilezikian JP, Rosen CJ. The effects of parathyroid hormone and alendronate alone or in combination in postmenopausal osteoporosis. N Engl J Med. 2003; 349:1207–1215. [PubMed: 14500804]

18. Eastell R, Lang T, Boonen S, Cummings S, Delmas PD, Cauley JA, Horowitz Z, Kerzberg E, Bianchi G, Kendler D, Leung P, Man Z, Mesenbrink P, Eriksen EF, Black DM. Effect of once-yearly zoledronic acid on the spine and hip as measured by quantitative computed tomography: results of the HORIZON Pivotal Fracture Trial. Osteoporos Int. 2010; 21:1277–1285. [PubMed: 19802508]

19. Lewiecki EM, Keaveny TM, Kopperdahl DL, Genant HK, Engelke K, Fuerst T, Kivitz A, Davies RY, Fitzpatrick LA. Once-monthly oral ibandronate improves biomechanical determinants of bone strength in women with postmenopausal osteoporosis. J Clin Endocrinol Metab. 2009; 94:171–180. [PubMed: 18840641]

20. Lang T, LeBlanc A, Evans H, Lu Y, Genant HK, Yu A. Cortical and trabecular bone mineral loss from the spine and hip in long-duration spaceflight. J Bone Miner Res. 2004; 19:1006–1012. [PubMed: 15125798]

21. Amin S, Kopperdhal DL, Melton LJ III, Achenbach SJ, Therneau TM, Riggs BL, Keaveny TM, Khosla S. Association of hip strength estimates by finite element analysis with fractures in women and men. J Bone Miner Res. 2011; 10

22. Johannesdottir F, Poole KE, Reeve J, Siggeirsdottir K, Aspelund T, Mogensen B, Jonsson BY, Sigurdsson S, Harris TB, Gudnason VG, Sigurdsson G. Distribution of cortical bone in the femoral neck and hip fracture: a prospective case-control analysis of 143 incident hip fractures; the AGES-REYKJAVIK Study. Bone. 2011; 48:1268–1276. [PubMed: 21473947]

23. Cody DD, Divine GW, Nahigian K, Kleerekoper M. Bone density distribution and gender dominate femoral neck fracture risk predictors. Skeletal Radiol. 2000; 29:151–161. [PubMed: 10794552]

24. Orwoll ES, Marshall LM, Nielson CM, Cummings SR, Lapidus J, Cauley JA, Ensrud K, Lane N, Hoffmann PF, Kopperdahl DL, Keaveny TM. Finite Element Analysis of the Proximal Femur and Hip Fracture Risk in Older Men. J Bone Miner Res. 2009; 24:475–483. [PubMed: 19049327]

25. Black DM, Bouxsein ML, Marshall LM, Cummings SR, Lang TF, Cauley JA, Ensrud KE, Nielson CM, Orwoll ES. Proximal femoral structure and the prediction of hip fracture in men: a large prospective study using QCT. J Bone Miner Res. 2008; 23:1326–1333. [PubMed: 18348697]

26. Bousson VD, Adams J, Engelke K, Aout M, Cohen-Solal M, Bergot C, Haguenauer D, Goldberg D, Champion K, Aksouh R, Vicaut E, Laredo JD. In vivo discrimination of hip fracture with quantitative computed tomography: results from the prospective European Femur Fracture Study (EFFECT). Journal of bone and mineral research. 2011; 26:881–893. [PubMed: 20939025]

27. Cheng X, Li J, Lu Y, Keyak J, Lang T. Proximal femoral density and geometry measurements by quantitative computed tomography: association with hip fracture. Bone. 2007; 40:169–174. [PubMed: 16876496]

28. Thomas CD, Mayhew PM, Power J, Poole KE, Loveridge N, Clement JG, Burgoyne CJ, Reeve J. Femoral Neck Trabecular Bone: Loss with Ageing and Role in Preventing Fracture. J Bone Miner Res. 2009

29. Bell KL, Loveridge N, Power J, Garrahan N, Stanton M, Lunt M, Meggitt BF, Reeve J. Structure of the femoral neck in hip fracture: cortical bone loss in the inferoanterior to superoposterior axis. J Bone Miner Res. 1999; 14:111–119. [PubMed: 9893072]
30. Crabtree N, Loveridge N, Parker M, Rushton N, Power J, Bell KL, Beck TJ, Reeve J. Intracapsular hip fracture and the region-specific loss of cortical bone: analysis by peripheral quantitative computed tomography. J Bone Miner Res. 2001; 16:1318–1328. [PubMed: 11450708]
31. Orwoll E, Blank JB, Barrett-Connor E, Cauley J, Cummings S, Ensrud K, Lewis C, Cawthon PM, Marcus R, Marshall LM, McGowan J, Phipps K, Sherman S, Stefanick ML, Stone K. Design and baseline characteristics of the osteoporotic fractures in men (MrOS) study--a large observational study of the determinants of fracture in older men. Contemp Clin Trials. 2005; 26:569–585. [PubMed: 16084776]
32. Barlow WE, Ichikawa L, Rosner D, Izumi S. Analysis of case-cohort designs. J Clin Epidemiol. 1999; 52:1165–1172. [PubMed: 10580779]
33. Yang L, Prevrhal S, McCloskey EV, Eastell R. A method to estimate femoral neck cortical thickness from clinical QCT scans (82). 2008:S181–S182.
34. Stephenson P, Seedhom BB. Modelling femoral curvature in the sagittal plane: a cadaveric study. Proc Inst Mech Eng H. 2001; 215:221–228. [PubMed: 11382081]
35. de Bakker PM, Manske SL, Ebacher V, Oxland TR, Cripton PA, Guy P. During sideways falls proximal femur fractures initiate in the superolateral cortex: evidence from high-speed video of simulated fractures. J Biomech. 2009; 42:1917–1925. [PubMed: 19524929]
36. Lotz JC, Cheal EJ, Hayes WC. Stress distributions within the proximal femur during gait and falls: implications for osteoporotic fracture. Osteoporos Int. 1995; 5:252–261. [PubMed: 7492864]
37. Manske SL, Liu-Ambrose T, de Bakker PM, Liu D, Kontulainen S, Guy P, Oxland TR, McKay HA. Femoral neck cortical geometry measured with magnetic resonance imaging is associated with proximal femur strength. Osteoporos Int. 2006; 17:1539–1545. [PubMed: 16847586]
38. Verhulp E, Van RB, Huiskes R. Load distribution in the healthy and osteoporotic human proximal femur during a fall to the side. Bone. 2008; 42:30–35. [PubMed: 17977813]
39. Holzer G, von SG, Holzer LA, Pichl W. Hip fractures and the contribution of cortical versus trabecular bone to femoral neck strength. J Bone Miner Res. 2009; 24:468–474. [PubMed: 19016592]
40. Thomas T, Feron JM, Delmas PD, Kaufman J, Tosi L, Cummings S, Lane J, Johnell O, Bouxsein ML. Optimal management of patients with stress fractures and the role of the orthopedic surgeon in reducing the risk of new fractures. Rev Chir Orthop Reparatrice Appar Mot. 2006; 92:165–174. [PubMed: 16800073]
41. Bell KL, Loveridge N, Power J, Garrahan N, Meggitt BF, Reeve J. Regional differences in cortical porosity in the fractured femoral neck. Bone. 1999; 24:57–64. [PubMed: 9916785]
42. Bell KL, Loveridge N, Power J, Rushton N, Reeve J. Intracapsular hip fracture: increased cortical remodeling in the thinned and porous anterior region of the femoral neck. Osteoporos Int. 1999; 10:248–257. [PubMed: 10525718]
43. Zebaze RM, Ghasem-Zadeh A, Bohte A, Iuliano-Burns S, Mirams M, Price RI, Mackie EJ, Seeman E. Intracortical remodelling and porosity in the distal radius and post-mortem femurs of women: a cross-sectional study. Lancet. 2010; 375:1729–1736. [PubMed: 20472174]
44. Cheng XG, Lowet G, Boonen S, Nicholson PH, Brys P, Nijs J, Dequeker J. Assessment of the strength of proximal femur in vitro: relationship to femoral bone mineral density and femoral geometry. Bone. 1997; 20:213–218. [PubMed: 9071471]
45. Moreland JD, Richardson JA, Goldsmith CH, Clase CM. Muscle weakness and falls in older adults: a systematic review and meta-analysis. J Am Geriatr Soc. 2004; 52:1121–1129. [PubMed: 15209650]
46. Nielson CM, Bouxsein ML, Freitas SS, Ensrud KE, Orwoll ES. Trochanteric soft tissue thickness and hip fracture in older men. J Clin Endocrinol Metab. 2009; 94:491–496. [PubMed: 19017753]
47. Lang T, Koyama A, Li C, Li J, Lu Y, Saeed I, Gazze E, Keyak J, Harris T, Cheng X. Pelvic body composition measurements by quantitative computed tomography: association with recent hip fracture. Bone. 2008; 42:798–805. [PubMed: 18234578]

48. Hangartner TN, Gilsanz V. Evaluation of cortical bone by computed tomography. J Bone Miner Res. 1996; 11:1518–1525. [PubMed: 8889852]

49. Prevrhal S, Fox JC, Shepherd JA, Genant HK. Accuracy of CT-based thickness measurement of thin structures: modeling of limited spatial resolution in all three dimensions. Med Phys. 2003; 30:1–8. [PubMed: 12557971]

50. Poole KE, Treece GM, Ridgway GR, Mayhew PM, Borggrefe J, Gee AH. Targeted regeneration of bone in the osteoporotic human femur. PLoS One. 2011; 6:e16190. [PubMed: 21264263]

Appendix

Our method of identifying cortical bone and estimating cortical thickness works on density images of cross sections of the proximal femur with the outer surface already segmented. The images were enlarged by 4 times using bilinear interpolation so that the pixel size was about 0.25 by 0.25 mm. For each cross section, density profiles perpendicular to the periosteal surface were generated at every other periosteal surface pixels, and the periosteal border k_p in the profile were identified. The maximum density D_{max} and the middle location k_{max} of $0.85D_{max}$ in the profile was then identified. If $D_{max}<0.2D_{FN}$ (D_{FN}: maximum density of the whole FN), which indicates a thin cortex, k_{max} is checked: if $k_p-k_{max}>2.5$ mm, k_{max} is adjusted so that $k_p-k_{max}=1.25$ mm. The endosteal border k_e is defined as the mirror point of k_p with respect to k_{max}, i.e., doubling the width of k_p-k_{max}. A five-point moving average filter was used to smooth the endosteal border points k_e in a cross section and the resulting points were connected to form a continuous endosteal border. The density profile was integrated from k_e to k_p (effectively calculated the bone mass) and divided by D_{FN} to derive the cortical thickness of the profile. The cortical thickness CtTh for the four quadrants was obtained by averaging the profile cortical thickness in the corresponding quadrants.

We validated the method of identifying cortical bone boundary on 3 female FN specimen scanned by a micro CT (μCT 100, SCANCO Medical AG, Brüttisellen, Switzerland) with a voxel size of $0.062\times0.062\times0.062$ mm^3. Eleven slices, evenly distributed from subcapital to distal FN, were selected from each specimen and analysed. We segmented the slice images for cortical region by threshold and manual tracing. We simulated clinical QCT scans of 1.0 mm pixel size by averaging the original micro CT images in 16-by-16 pixel blocks and applied our method for cortical segmentation (Figure 6). The reasons for simulating rather than performing clinical QCT were that scanning would introduce more variables such as positioning and region-of-interest definition which were beyond the merit of this validation exercise. We calculated cortical, trabecular and integral areas and vBMDs and cortical thickness in the 4 quadrants for both micro CT and simulated QCT images and compared the results (Table 6). Taking micro CT results as standard, largest errors were found in cortical compartments, particularly in the 2 superior quadrants (supero-anterior and supero-posterior) where cortex was thin. Our method over-estimated cortical area in the 2 superior quadrants by about 20%. On average, cortical area of the superior quadrants of the FN in this validation study was 23 mm^2 and a 20% error in the area represented only 5 pixels in the simulated clinical CT that were misclassified as cortical. Our method under-estimated cortical vBMD by 33–37% in the superior quadrants, which was expected since measurement of vBMD has been shown to decrease with QCT resolution and cortical thickness by as much as 60% [48,49]. Our method over-estimated cortical thickness by 6–10%, and this compared very favourably with errors of up to 100% for sub-millimetre thickness by methods based on density [48,49]. Considering that the resolution of clinical QCT is 16 times lower than the micro CT used here, we regarded our cortical segmentation method reliable and valid.

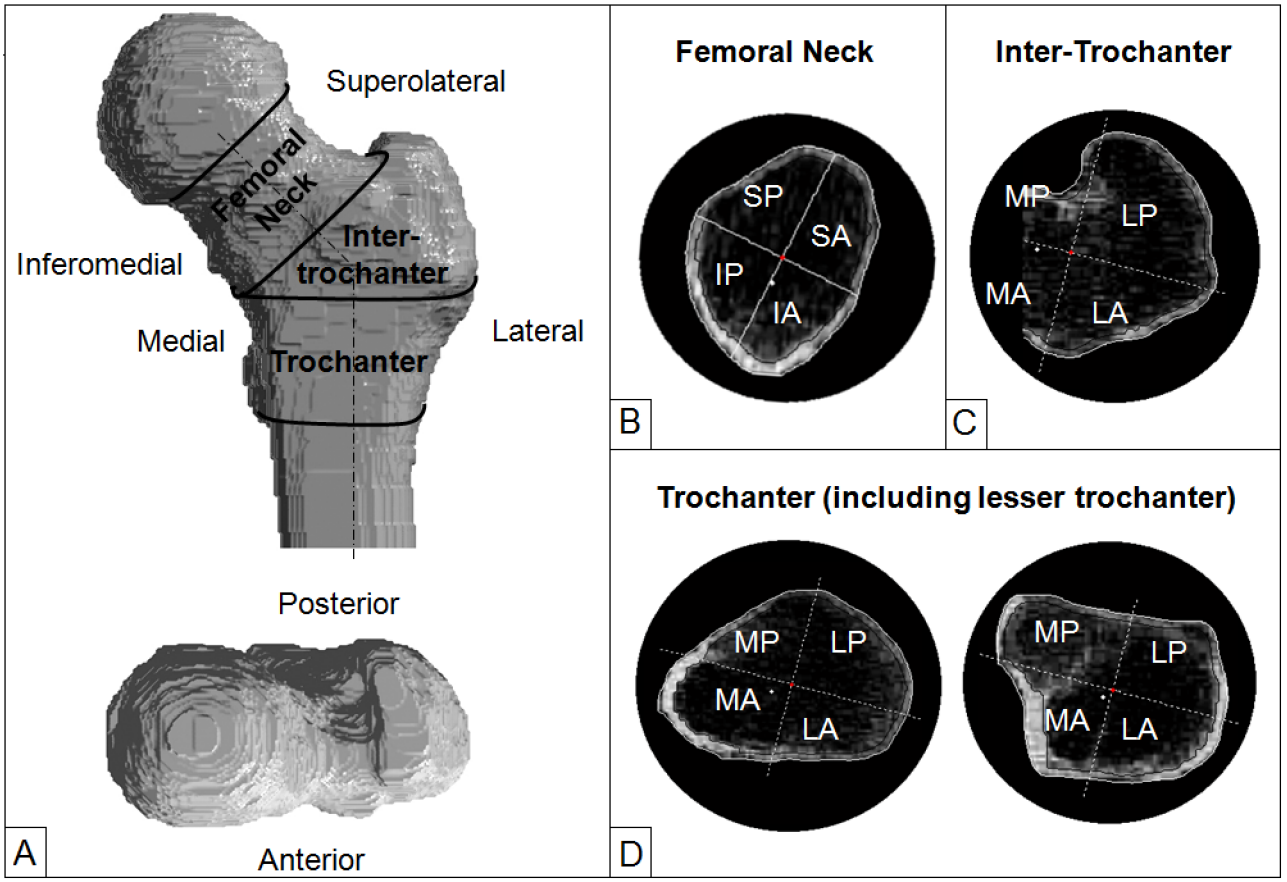

Figure 1.

(A) Regions of interest for analysis of volumetric BMD and cortical thickness in the proximal femur. (B) Quadrants of cross sections in the femoral neck. IA: infero-anterior; IP: infero-posterior; SA: superoanterior; SP: supero-posterior. (C) Quadrants of cross sections in the intertrochanter. Notice that the cross sections are not complete medially since it is bounded by the femoral neck; (D) Quadrants of cross section in the trochanter: left image shows a cross section in the proximal trochanter and right image a cross section at the lesser trochanter. The black lines inside the bone cross sections separate cortical and trabebular bone. MA: medio-anterior; LA: latero-anterior; MP: medio-posterior; SP: supero-posterior.

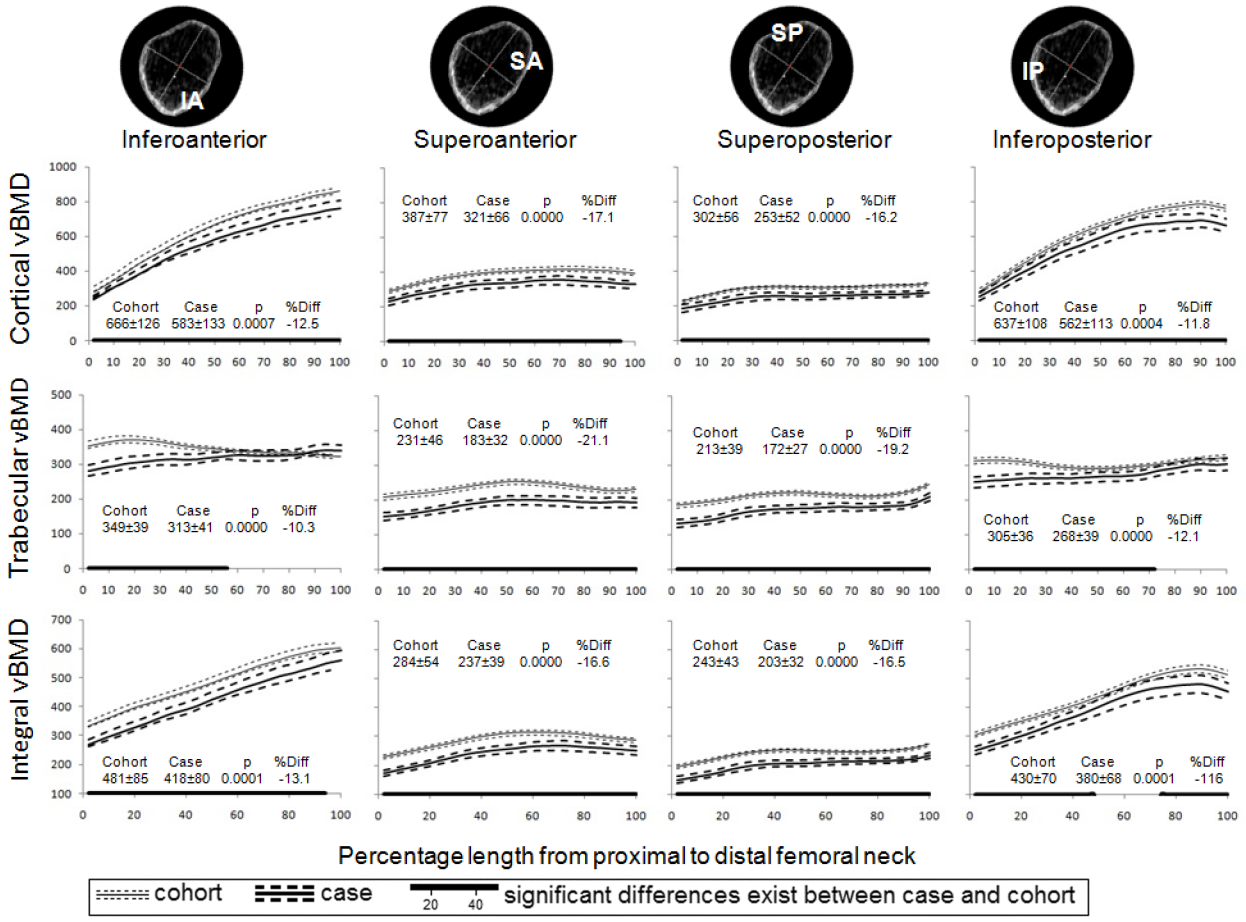

Figure 2.

Mean (95% CI) cortical, trabecular and integral vBMD (mg/cm^3) along the femoral neck by quadrant and fracture status. The numbers represent the mean ± standard deviation over the entire length, the t-test p value for comparison of means and percentage difference in means.

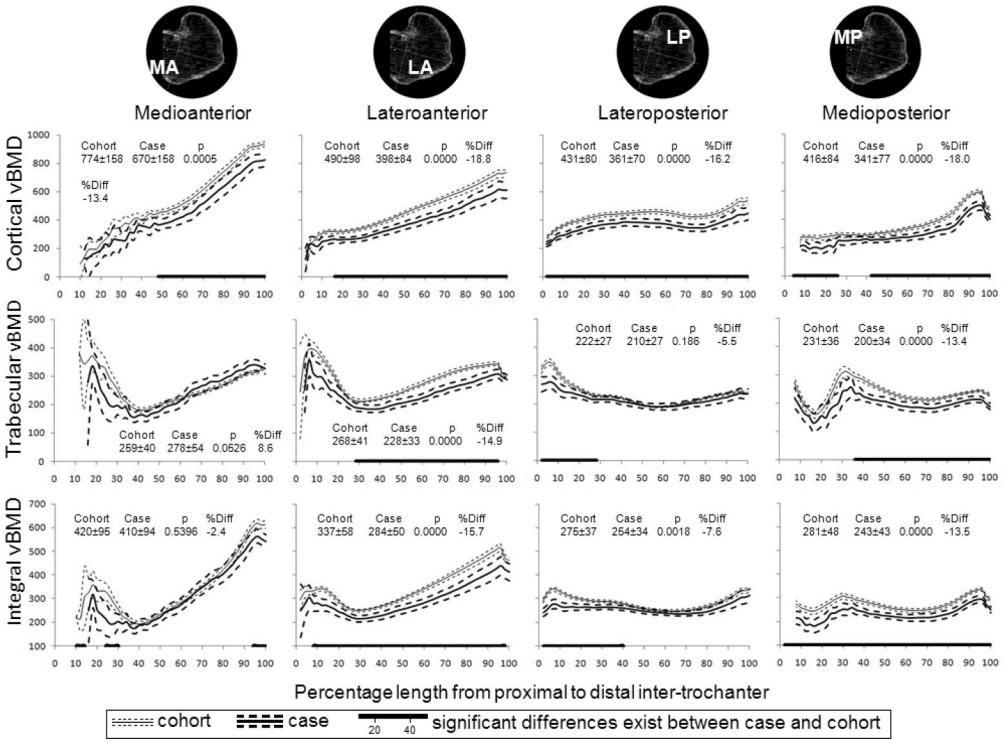

Figure 3.

Mean (95% CI) cortical, trabecular and integral vBMD (mg/cm^3) along the intertrochanter by quadrant and fracture status. The numbers represent the mean ± standard deviation over the entire length, the t-test p value for comparison of means and percentage difference in means.

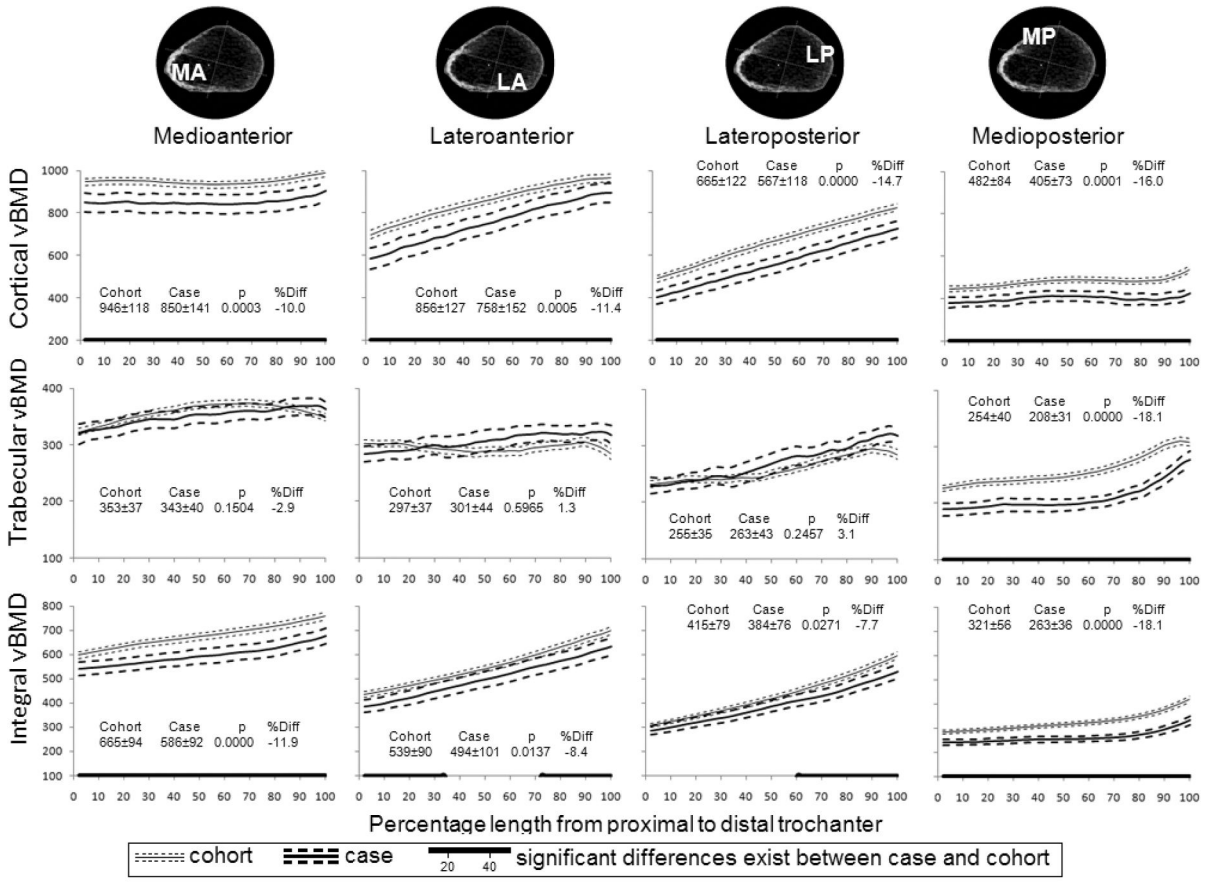

Figure 4.

Mean cortical, trabecular and integral vBMD (mg/cm^3) along the trochanter by quadrant and fracture status. The numbers represent the mean ± standard deviation over the entire length, the t-test p value for comparison of means and percentage difference in means.

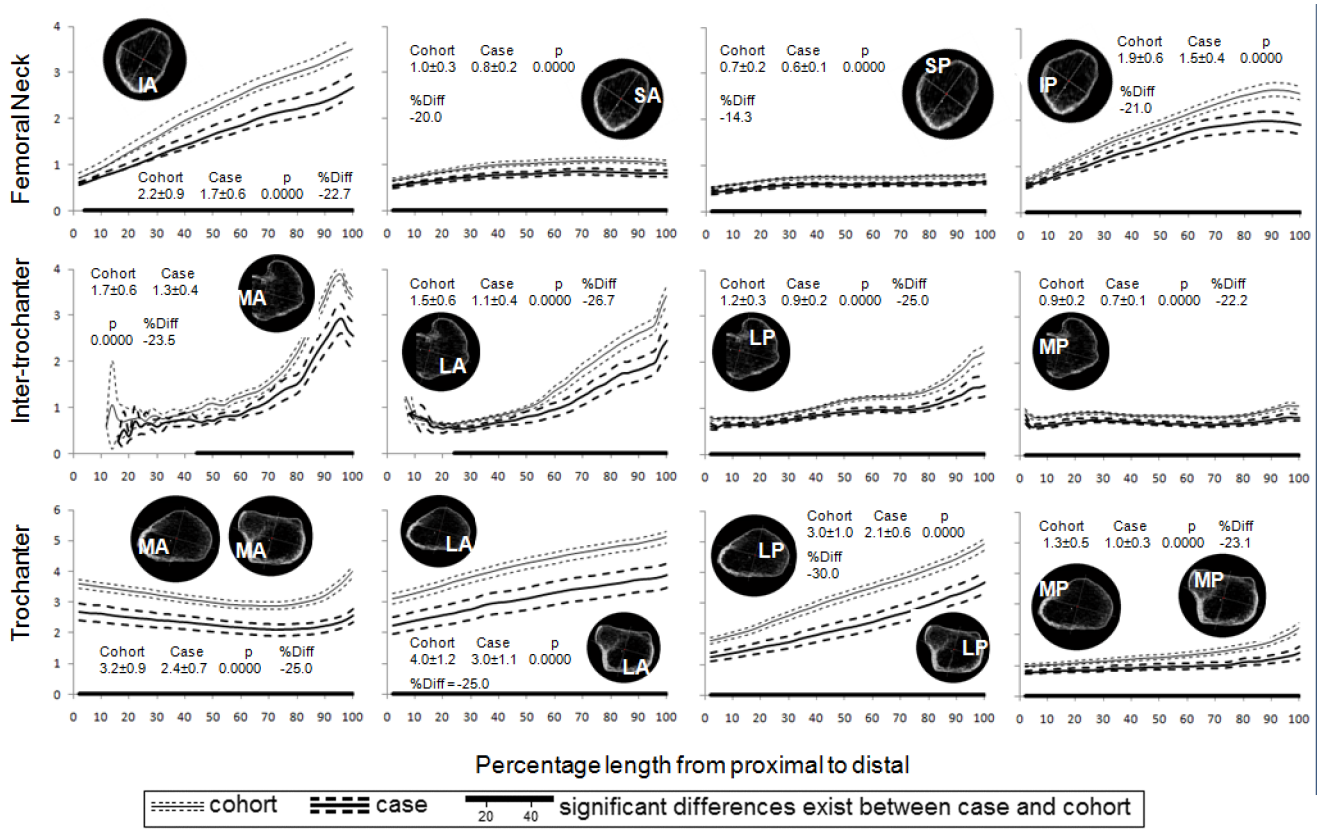

Figure 5.

Mean (95% CI) cortical thickness (mm) along the femoral neck, intertrochanter and trochanter by quadrant and fracture status. The numbers represent the mean ± standard deviation over the entire length, the t-test p value for comparison of means and percentage difference in means.

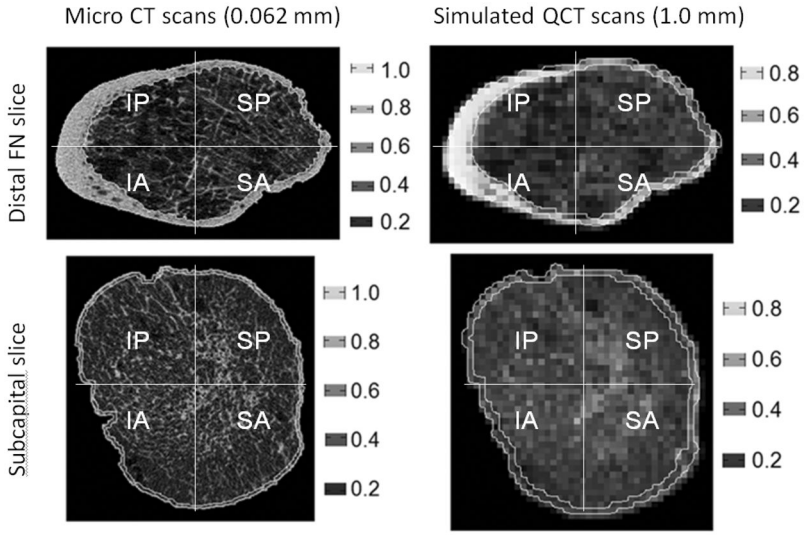

Figure 6.
Typical micro CT images of the (A) distal femoral neck and (C) subcapital and the corresponding simulated clinical QCT images (B) and (D). Note the similarity in cortical region between the micro CT and simulated clinical QCT.

Table 1

Intra-observer reproducibility of vBMD (%CV)

	Cortical vBMD	Trabebular vBMD	Integral vBMD	Cortical thickness	CSA	PMI
FN						
Inferomedial	2.0	1.5	1.8	4.9	-	-
Anterior	0.9	1.6	0.9	2.7	-	-
superolateral	0.8	2.4	1.0	1.8	-	-
Posterior	2.0	2.6	2.1	3.9	-	-
Total	1.2	1.2	1.2	-	0.9	6.5
Inter-trochanter						
Medial	2.1	2.5	2.2	4.3	-	-
Anterior	1.2	1.2	1.1	1.7	-	-
Lateral	1.0	0.7	0.6	1.1	-	-
Posterior	2.9	1.5	2.0	1.2	-	-
Total	0.8	0.6	0.6	-	1.0	3.3
Trochanter						
Medial	1.4	1.7	1.2	1.8	-	-
Anterior	1.4	1.8	1.7	3.6	-	-
Lateral	2.0	2.0	1.9	3.0	-	-
Posterior	1.0	1.7	1.0	1.6	-	-
Total	0.8	1.2	0.9	-	0.6	4.6
Total Hip	0.7	0.5	0.6	-	-	-

Table 2

Comparison of baseline characteristics

	Case group (n=38)	Sub-cohort (n=212)	Full MrOS (n=5995)
Age (yr)	78.6 (6.0)[c]	73.2 (5.6)	73.7 (5.9)
Height (cm)	172.4 (5.8)	174.5 (7.5)	174.1 (6.8)
Weight (kg)	78.4 (12.7)[a]	83.5 (13.5)	83.1(13.3)
BMI (kg/m^2)	26.3 (3.3)	27.3 (3.6)	27.4 (3.8)
TH aBMD (g/cm^2)	0.79 (0.12)[c]	0.95 (0.13)	0.96 (0.14)

Note: Values marked with a, b, c indicate a significant difference between cases and subcohort ($p<0.05$, 0.005 and 0.0005).

Table 3

Hazard ratio (95% CI) for one standard deviation decrease in vBMD and cortical thickness (adjusted for age, BMI and study site)

	Infero-medial Femoral Neck	**Medial Intertrochanter**	**Medial Trochanter**	
Cortical vBMD	1.98 (1.26, 3.10)	2.28 (1.44, 3.63)	2.01 (1.26, 3.20)	
	p=0.0030	p=0.0005	p=0.0034	
Trabecular vBMD	4.65 (2.64, 8.20)	2.33 (1.27, 4.26)	6.91 (3.11, 15.35)	
	p<0.0001	p=0.0060	p<0.0001	
Integral vBMD	2.83 (1.71, 4.67)	2.17 (1.34, 3.53)	3.70 (2.04, 6.71)	
	p<0.0001	p=0.0017	p<0.0001	
Cortical thickness	2.89 (1.65, 5.05)	3.18 (1.74, 5.81)	3.44 (1.70, 6.98)	
	p=0.0002	p=0.0002	p=0.0006	
	Supero-lateral Femoral Neck	*Lateral Intertrochanter*	*Lateral Trochanter*	
Cortical vBMD	2.87 (1.55, 5.30)	3.45 (1.90, 6.26)	2.60 (1.44, 4.70)	
	p=0.0008	p<0.0001	p=0.0015	
Trabecular vBMD	5.45 (2.85, 10.44)	2.80 (1.61, 4.84)	1.00 (0.64, 1.55)	
	p<0.0001	p=0.0002	p=0.9874	
Integral vBMD	3.90 (2.12, 7.16)	2.71 (1.56, 4.71)	1.86 (0.96, 3.60)	
	p<0.0001	p=0.0004	p=0.0651	
Cortical thickness	5.13 (1.91, 13.72)	3.68 (1.77, 7.66)	2.60(1.54, 4.38)	
	p=0.0011	p=0.0005	p=0.0004	
	Femoral Neck	*Intertrochanter*	*Trochanter*	*Total hip*
Cortical vBMD	2.36 (1.46, 3.82)	3.09 (1.80, 5.30)	2.45 (1.45, 4.12)	2.61 (1.60, 4.27)
	p=0.0005	p<0.0001	p=0.0008	p=0.0001
Trabecular vBMD	6.54 (3.35, 12.77)	4.02 (2.01, 8.05)	2.74 (1.43, 5.29)	4.92 (2.55, 9.50)
	p<0.0001	P<0.0001	p=0.0025	p<0.0001
Integral vBMD	3.34 (1.95, 5.71)	2.86 (1.68, 4.86)	3.53 (1.87, 6.67)	3.23 (1.82, 5.72)
	p<0.0001	p=0.0001	p=0.0001	p<0.0001
Cortical thickness	3.49 (1.82, 6.71)	3.67 (1.86, 7.25)	3.09 (1.69, 5.66)	2.54 (1.59, 4.05)
	p=0.0002	p=0.0002	p=0.0003	p<0.0001
Cross section area	1.10 (0.76, 1.58)	1.07 (0.65, 1.74)	1.05 (0.65, 1.70)	
	p=0.6260	p=0.7901	p=0.8373	
PMI	2.73 (1.43, 5.20)	2.35 (1.27, 4.33)	1.45 (0.94, 2.23)	
	p=0.0022	p=0.0063	p=0.0958	

PMI: Polar moment of inertia.

Table 4

Hazard ratio (95% CI) for one standard deviation decrease in vBMD and cortical thickness (adjusted for age, BMI, study site and hip aBMD)

	Infero-medial Femoral Neck	**Medial Intertrochanter**	**Medial Trochanter**	
Cortical vBMD	1.31 (0.66, 2.57)	1.29 (0.70, 2.39)	1.09 (0.63, 1.87)	
Trabecular vBMD	*3.44 (1.77, 6.69)	1.81 (0.82, 3.99)	*6.20 (2.71, 14.18)	
Integral vBMD	1.99 (1.06, 3.75)	1.21 (0.65, 2.27)	1.99 (1.01, 3.93)	
Cortical thickness	1.82 (0.91, 3.63)	1.26 (0.57, 2.77)	1.86, 0.87, 3.94)	
	Supero-lateral Femoral Neck	*Lateral Intertrochanter*	*Lateral Trochanter*	
Cortical vBMD	1.38 (0.66, 2.90)	1.76 (0.81, 3.82)	1.29 (0.58, 2.87)	
Trabecular vBMD	*3.21 (1.65, 6.24)	1.72 (0.89, 3.34)	1.73 (0.96, 3.09)	
Integral vBMD	2.03 (1.04, 3.97)	1.57 (0.81, 3.05)	1.42 (0.67, 3.03)	
Cortical thickness	1.55 (0.50, 4.81)	1.93 (0.84, 4.45)	1.25 (0.61, 2.57)	
	Femoral Neck	*Intertrochanter*	*Trochanter*	*Total hip*
Cortical vBMD	1.41 (0.74, 2.70)	1.62 (0.81, 3.27)	1.20 (0.62, 2.32)	1.19 (0.61, 2.33)
Trabecular vBMD	*4.27 (2.00, 9.08)	2.44 (1.05, 5.68)	*4.08 (1.88, 8.87)	*3.89 (1.83, 8.30)
Integral vBMD	2.11 (1.10, 4.03)	1.63 (0.86, 3.08)	1.93 (0.96, 3.88)	1.67 (0.87, 3.18)
Cortical thickness	1.88 (0.89, 3.97)	1.69 (0.75, 3.80)	1.52 (0.72, 3.24)	1.49 (0.85, 2.61)
Cross section area	0.95 (0.62, 1.48)	0.97 (0.54, 1.72)	0.68 (0.89, 1.56)	
PMI	2.66 (1.08, 6.56)	1.52 (0.68, 3.44)	0.98 (0.63, 1.52)	

*HR is significant at p<0.001; PMI: polar moment of inertia.

Table 5

Side differences (95% CI) in QCT measures for men with incident hip fracture (non-fractured side minus fractured side)

	Infero-medial Femoral Neck	**Medial Intertrochanter**	**Medial Trochanter**	
Cortical vBMD	−14 (−64, 34)	−11 (−55, 33)	6 (−45, 58)	
Trabecular vBMD	−4 (−20, 12)	0 (−13, 14)	−4 (−15, 7)	
Integral vBMD	−9 (−39, 20)	−3 (−24, 19)	0 (−25, 24)	
Cortical thickness	0.0 (−0.2, 0.1)	−0.0 (−0.1, 0.1)	−0.0 (−0.2, 0.2)	
	Supero-lateral Femoral Neck	*Lateral Intertrochanter*	*Lateral Trochanter*	
Cortical vBMD	7 (−19, 32)	−4 (−35, 26)	4 (−54, 62)	
Trabecular vBMD	5 (−9, 18)	−3 (−14, 8)	0 (−16, 16)	
Integral vBMD	4 (−11, 20)	−4 (−20, 11)	−2 (−40, 35)	
Cortical thickness	−0.0 (−0.0, 0.1)	−0.0 (−0.1, 0.1)	−0.0 (−0.4, 0.4)	
	Femoral Neck	*Intertrochanter*	*Trochanter*	*Total hip*
Cortical vBMD	−5 (−42, 32)	−6 (−39, 27)	5 (−46, 57)	1 (−38, 41)
Trabecular vBMD	−2 (−14, 10)	−2 (12, 9)	−2 (−12, 7)	−2 (−11, 7)
Integral vBMD	−4 (−25, 16)	−4 (−20, 12)	0 (−27, 26)	−2 (−20, 16)
Cortical thickness	−0.0 (−0.1, 0.1)	−0.0 (−0.1, 0.1)	−0.0 (−0.3, 0.2)	−0.0 (−0.2, 0.2)
Cross section area	−38 (−117, 42)	−52 (−182, 77)	−94 (−222, 34)	
PMI	−4.9 (−12, 2)	−31 (−124, 63)	−19 (−69, 31)	

vBMD in mg/cm^3, cortical thickness in mm, cross section area in mm^2 and polar moment of inertia (PMI) in cm^4.

J Bone Miner Res. Author manuscript; available in PMC 2013 November 01.

Table 6

Results of validation study

	Area			***vBMD***			***Cortical***
	Cortical	***Trabecular***	***Integral***	***Cortical***	***Trabecular***	***Integral***	***thickness***
	Mean (95% CI) values from μCT						
IA	42 (38, 46)	192 (174, 210)	234 (218, 249)	.64 (.60, .68)	.23 (.22, .25)	.32 (.31, .32)	1.7 (1.6, 1.9)
SA	21 (19, 22)	212 (205, 219)	233 (226, 240)	.59 (.56, .62)	.21 (.20, .21)	.24 (.24, .25)	0.9 (0.9, 1.0)
SP	24 (22, 26)	213 (197, 229)	237 (221, 253)	.61 (.58, .64)	.21 (.20, .22)	.25 (.24, .26)	1.0 (1.0, 1.1)
IP	41 (36, 46)	193 (183, 203)	234 (226, 242)	.64 (.61, .67)	.23 (.22, .24)	.30 (.30, .31)	1.7 (1.5, 1.9)
Total	127 (117, 139)	834 (784, 884)	962 (917, 1008)	.63 (.59, .66)	.22 (.21, .23)	.28 (.28, .29)	1.0 (1.3, 1.5)
	Mean (95% CI) percentage differences (100(QCT-μCT)/μCT)						
IA	−6 (−13, 0)	2 (1, 3)	−1 (−1, 0)	−17 (−20, −13)	7 (5, 9)	−4 (−4, −4)	6 (0, 12)
SA	22 (15, 28)	−3 (−3, −2)	−1 (−1, −1)	−37 (−39, −35)	2 (2, 3)	−5 (−6, −5)	1 (4, 7)
SP	18 (8, 29)	−2 (−3, −2)	−1 (−1, −1)	−33 (−35, −30)	3 (2, 4)	−5 (−5, −5)	6 (0, 13)
IP	−1 (−8, 6)	1 (0, 2)	−1 (−1, 0)	−18 (−21, −14)	6 (4, 8)	−4 (−4, −3)	10 (5, 14)
Total	4 (−3, 11)	2 (1, 2)	1 (1, 2)	−24 (−26, −22)	5 (4, 6)	−3 (−3, −3)	6 (2, 11)

Units of mean value from μCT: Area in mm^2, vBMD in g/cm^3 and cortical thickness in mm.

IA: Infero-anterior; SA: Supero-anterior; SP: Supero-posterior; IP: Infero-posterior;